SSC11-VI-2

Pre-launch Optical Characteristics of the Oculus-ASR Nanosatellite for Attitude and Shape Recognition Experiments

Lyon B. King and Philip Hohnstadt
Michigan Technological University
Department of Mechanical Engineering – Engineering Mechanics
1400 Townsend Drive, Houghton, MI 49931
lbking@mtu.edu

Kelly Feirstine
Schafer Corporation
2309 Renard Place SE, Suite 300, Albuquerque, NM 87106; (505) 338-2867
kfeirstine@schaferalb.com

ABSTRACT

Most all objects in Earth orbit, when imaged using all but the largest ground-based telescopes, appear as unresolved point sources of light. Although these unresolved images are featureless it may be possible to determine parameters related to an object's attitude and/or rotation rate by analyzing the spectral and temporal content of reflected sunlight. For instance a faceted rotating object may produce a periodic cycle of bright glints or a spectrally distinct surface coating may be detectable using a spectrometer. The Oculus-ASR is a 50-kg-class nanosatellite specifically designed to exercise and validate techniques for determining an orbiting object's pose using unresolved ground imagery. The nanosatellite has been optically characterized in an AFRL ground facility to determine reflective signatures that can be expected on orbit. Once on orbit, the Oculus-ASR will be monitored by ground-based telescopes and these observations will be reconciled against 'truth' attitude data recorded during various maneuvers. This paper reports on the basic design of the spacecraft, summarizes the concept of operations, and presents results of the pre-launch optical ground characterization.

INTRODUCTION

As access to space has become more common, the number of objects orbiting Earth has increased drastically. Some of these objects are functional satellites that perform vital operations for commercial or military purposes. However, many of the objects orbiting Earth are debris made up of defunct satellites, spent rocket stages, and ruins of satellites destroyed in anti-satellite weapon tests or collisions. These objects pose a growing threat to functional satellites. Collisions with orbital debris can cause damage to essential commercial and military assets that would render them useless. Therefore, it is beneficial for the space community to have an accurate knowledge of current and future locations of orbiting objects. The effort to identify, catalog, and track the objects orbiting Earth, both functional and nonfunctional, is part of the overall Space Situational Awareness (SSA) activity.

Ground-based optical telescopes are one key instrument in achieving SSA. In addition to determining the trajectory of an orbiting object, optical telescopes can also be used to determine the object's attitude, physical profile, and features. A drawback of using optical telescopes for such Attitude and Shape Recognition (ASR) is the fundamental limitation of resolvability. Orbiting objects become unresolvable at high orbits or small telescope apertures. In fact, many orbiting objects fall outside the resolvable range of most ground-based telescopes. Under these conditions, a telescope sees the object as a point-source of light and it is impossible to distinguish features of the object from the telescope image.

While spatial features cannot be determined from unresolved 'dots' of light, these dots contain spectral and photometric information that can be used to deduce properties of the object. Using unresolved imagery to observe and characterize orbiting objects with the goal of determining their attitude and detecting configuration changes (e.g. deployments) is important. This is accomplished by analyzing the spectral frequencies and temporal changes in the intensity contained in the point-source of light and referencing the measured signals with known spectral signatures. If successful, this technique could lead to an inexpensive network of sensors with broad coverage.

Given an orbiting object with known optical properties it is relatively straightforward to predict the observed signature if the object's attitude or maneuver is specified. This paper focuses on the inverse problem: given a measured optical signature generated by an object with known properties is it possible to calculate the object's attitude? While, in principle, this problem can be addressed the algorithms are non-trivial and require validation and/or calibration. Calibration opportunities are rare as they require pre-characterization or at least optical modeling of the orbiting object to create a signature database prior to launch.

OCULUS-ASR

The Oculus-ASR is a nanosatellite being developed through a collaboration between Michigan Technological University (MTU) and AFRL. The Oculus-ASR's mission is to provide calibration opportunities for ground-based observers attempting to validate and/or anchor algorithms capable of determining spacecraft attitude and configuration using unresolved optical imagery. The optical signature of the vehicle has been extensively characterized in ground facilities; the Results section of this paper describes the results of these tests in detail. Once on orbit the Oculus-ASR will serve as a cooperative imaging target for ground-based telescopes. Ground controllers at MTU will command the vehicle to perform various attitude maneuvers during overflights of these telescopes. After each ground-viewing opportunity the MTU team will provide attitude truth history to the telescope observers for comparison with their findings.

The Oculus-ASR nanosatellite has been designed and built by MTU undergraduate students. In January 2011 the Oculus-ASR team won the sixth University Nanosatellite Program competition (UNP). The UNP is a national, university-level competition run by the Air Force Research Laboratory and funded by the Air Force Office of Scientific Research. As the winner of this competition, the Oculus-ASR team will receive follow-on support for flight preparation from AFRL staff.

Vehicle Overview

Oculus-ASR is a 70-kg satellite with a volume envelope of 50 cm by 50 cm by 80 cm. It consists of two modules that are permanently attached. An octagonal module, referred to as the Oculus module, sits atop a square module, known as the ASR module. Figure 1 shows the assembled vehicle and identifies the major features on the exterior of the satellite.

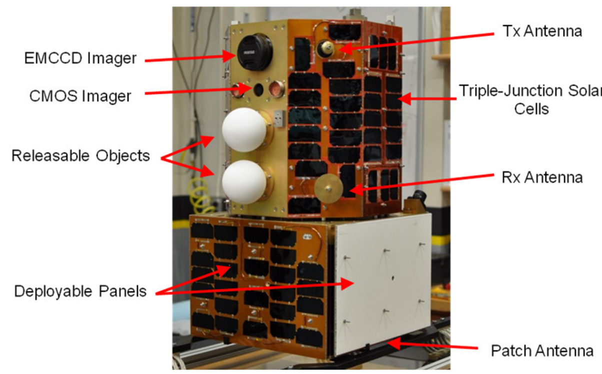

Figure 1: The Oculus-ASR vehicle

Each of the four sides on the ASR module has a deployable panel. Three of these panels are covered in solar cells. The fourth is covered in Duraflect material. Duraflect is a highly reflective, diffuse white coating used as an optical standard for characterization and calibration measurements. Under and on the back of each deployable panel are specific materials requested by telescope operators for their distinct spectral characteristics. These materials are red, blue, yellow, and clear anodized aluminum. Each panel is deployed separately through the actuation of Frangibolt actuators. Spring-loaded hinges then lift the panel until it locks in place 90° from its undeployed position. These deployable panels allow the spectral signature of Oculus-ASR to be changed multiple times over the course of the mission by altering the vehicle's shape and exposed materials.

Two releasable objects are mounted to the Oculus module. These objects are approximately 10 cm in diameter and will be used to provide ground observers an opportunity to view small, closely spaced objects. The releasable objects are coated in the same Duraflect material used on the deployable panel, and can be released individually using the same style of Frangibolt actuator used for the deployable panels. These objects then drift from the vehicle due to the force exerted from the actuator.

The satellite is capable of 3-axis attitude determination and control. This allows Oculus-ASR to perform a wide variety of attitude maneuvers for telescope calibration purposes. Attitude determination is accomplished using a Bartington Mag-03MRN magnetometer and three Silicon Sensing SiRRS01-05 gyroscopes. These sensors provide an attitude reading accurate to within 5 degrees of error. Three reaction wheels and three magnetic torque rods are used to control the vehicle's attitude. Both reaction wheels and torque rods were developed in-house at Michigan Technological University. Each magnetic torque rod can generate approximately 285 μN·m of torque. A single reaction wheel is capable of 11 mN·m of torque. The reaction wheels allow the vehicle to achieve an angular velocity of 7.5 °/s on its x- and y- axes and up to 17 °/s on its z axis.

Concept of Operations

Oculus-ASR will exercise three key capabilities of telescopes using unresolved optical imagery: determine the spacecraft's attitude, detect configuration changes, and measure the change in signature due to a small resident space object in close vicinity to the main vehicle.

On-orbit, one of Oculus-ASR's roles will be to fulfill requests to view specific attitude profiles during overpasses of the observatory. These attitude profiles are described with regards to a body coordinate system (BCS) and an orbital coordinate system. Figures 2 depicts these coordinate systems.

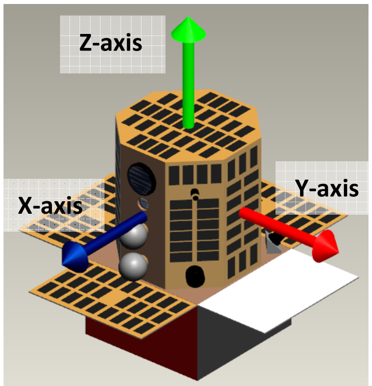

(a)

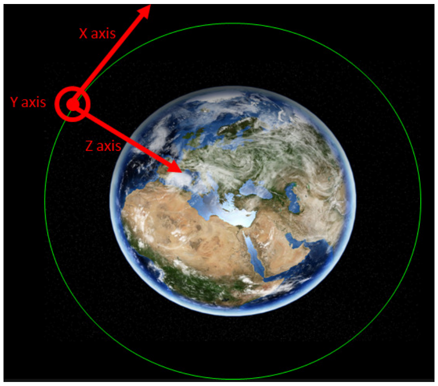

(b)

Figure 2: Body Coordinate System (a) and Orbital Coordinate System (b) used to define the attitude of Oculus-ASR

Telescope operators may select maneuvers from a list of predetermined attitude profiles. These include:

<u>Ready:</u> Rotation rate about any axis is less than 2 °/s; the angles between the BCS and Orbital Coordinate System are uncontrolled

<u>Fixed-Axis Rotation:</u> Any single body coordinate axis is fixed with respect to the Orbital Coordinate System; constant rotation rate about the fixed axis, no rotation about any other axis.

<u>Earth Pointing:</u> A vector in the BCS is kept pointed at a fixed location on the Earth's surface.

<u>Orbital Coordinate System Fixed Attitude:</u> Constant angles between the BCS and Orbital Coordinate System with zero rotation; attitude is constant with respect to the Orbital Coordinate System

<u>Sun Pointing:</u> A vector in the BCS is kept pointed at the Sun.

Observatories will schedule these maneuvers with the operators of Oculus-ASR in advance of an observation opportunity. At all times, Oculus-ASR will be recording a time-indexed history of its attitude. After an overpass maneuver, this attitude history will be downloaded to the MTU ground station, where it will be delivered to the telescope operators. Telescope operators will then be able to use the truth attitude from the vehicle and the models developed through the ground characterization of the vehicle to determine if the telescope was providing readings accurate enough to determine Oculus-ASR's attitude during the observation.

Oculus-ASR is also capable of changing its physical configuration through the use of deployable panels.

Deployment of a panel changes both the projected profile of the vehicle and the exposed materials on the exterior of the vehicle. Each panel exposes a spectrally distinct material. There are a total of four deployable panels on the satellite, which can be deployed individually to provide four distinct changes in Oculus-ASR's physical configuration. Once deployed the panels cannot be retracted. After establishing baseline measurements of the vehicle in its as-launched configuration, telescope operators will request the deployment of a panel. The operators of Oculus-ASR will command the deployment and confirm the successful opening of a panel. Telescope operators can then take further measurements and compare these to the baseline measurements in order to determine which panel was opened and when the actuation occurred.

Finally, Oculus-ASR is equipped with two releasable objects. These objects are much smaller than Oculus-ASR. After an object is released, it drifts slowly from the vehicle. The goal of the telescope operators is to determine if and when this small object can be detected and distinguished from the Oculus-ASR. The ideal method of accomplishing this will be to release the object at the beginning of the first of two consecutive overpasses of an observatory. This gives telescope operators an additional opportunity to view the satellite and the separated object in the event that the separation cannot be detected during the first observation opportunity.

Vital to all of these operations is having a complete radiometric characterization of the vehicle prior to launch. This characterization yields models that can be used as truth values to which the experimental measurements taken from the telescopes can be compared.

PRE-LAUNCH CHARACTERIZATION

SSA relies not only on measurements of space objects but on an understanding of what those measurements mean. In order to understand the signatures of space objects, it is necessary to measure, model, and simulate the spatial characteristics of spacecraft. One of the objectives of the Oculus-ASR characterization experiment was to provide ground-truth satellite data for the construction and validation of predictive computer models such as those used in Time-domain Analysis Simulation for Advanced Tracking (TASAT), a satellite modeling code used throughout the SSA community. Another objective of this experiment is to establish if pose determination is possible solely from on-orbit spectral returns. Imaging the satellite on the ground will help ascertain whether or not this objective can be met.

Multispectral optical measurements of the Oculus-ASR satellite were conducted at an Air Force Research Laboratory (AFRL) far-field optical measurement facility by an AFRL program. This facility allows accurately simulated observations of space objects without significant atmospheric effects. This ability provides the opportunity to measure the optical signatures of satellites and then modify corresponding satellite models to improve agreement with these ground-truth optical signatures. This characterization experiment obtained accurate far-field imagery, Optical Cross Section (OCS), and spectral-polarimetric glint and off-glint data helpful in validating remote observations.

The use of anodized colored panels on the Oculus-ASR satellite base was intended for the purpose of inferring satellite pose or attitude from observations. Satellite imagery for typical on-orbit viewing geometries will not be resolved. In certain poses, when the satellite is observed from the ground, metallic glints or non-colored panel reflections will often dominate the OCS and mask the colored panel contributions. It is important to understand which spectral filtered wavebands will contribute the most attitude information. Common astronomical filters are V-band (550nm center wavelength with a nominal full width half maximum specification of 90nm), and I-band (800nm center wavelength with a nominal full width half maximum specification of 150nm); often, these bands along with broadband images are obtained. The Oculus-ASR ground-truth characterization acquired broadband, V-band, I-band, and 650nm narrow band (10nm bandpass) filtered images as well as spectral data spanning the 350nm – 2500nm wavelength range.

FAR-FIELD OPTICAL MEASUREMENTS

The next sections describe the scientific equipment used at the optical facility, the geometries at which Oculus-ASR data was collected, and the measurement and analysis approach.

Imaging Equipment

A digital scientific imaging camera called the PIXIS provides 16-bit data from 400nm – 900nm. Filtered waveband images are acquired with the PIXIS at 4 wavebands; V-band (550nm center wavelength with a nominal full width half maximum specification of 90nm), I-band (800nm center wavelength with a nominal full width half maximum specification of 150nm), 650nm waveband with 10nm bandpass, and broadband. An Analytical Spectral Devices spectro-radiometer (ASD) is used during the data collects as well. The ASD provides continuous spectral information from 350nm – 2500nm. A 6-DOF robotic arm was used to pose the satellite.

Accurate far-field measurements rely on a reference material in the scene with the satellite. Troublesome atmospheric variations and absorption lines fall out of the measurements when measurement images can be normalized to a known reference image under the same lighting conditions. Solar passive satellite surface radiance can vary anywhere from 0.1 times the radiance of Spectralon for a dark paint to 50,000 times for a smooth metallic glint. A reference material that exhibits the same brightness independent of illumination and surface orientation and one that is spectrally flat over the entire measurement wavelength range would be ideal. The reference should also have an OCS comparable to that of Oculus-ASR. Spectralon is a good diffuse reference for off-glint satellite geometries, though it has a limited range of acceptance angles and exhibits enhanced backscatter in a monostatic geometry. A 6"x6" smooth glass panel is spectrally flat and so is used as a reference for most of the Oculus-ASR ground-truth characterization experiment. The glass reference provides a directed signal that is not subject to background light.

Oculus-ASR Imaging Geometries

Oculus-ASR PIXIS images were obtained in a bistatic (BIS) or 90° solar phase angle geometry which simulates Earth terminator conditions, as shown in **Error! Reference source not found.**. The satellite was posed in 10 different positions and rotated about each position. Multiple filtered waveband images were taken at each position. **Error! Reference source not found.** describes each position, the rotations done in each position, and the wavebands acquired at each position. The spin axis, or nadir pointing axis, is given in terms of azimuth (AZ) and elevation (EL), where 0°EL is opposite the illumination vector and the sensor vector is -90°AZ. The horizontal plane (0°EL) is defined by the illumination vector and the sensor vector.

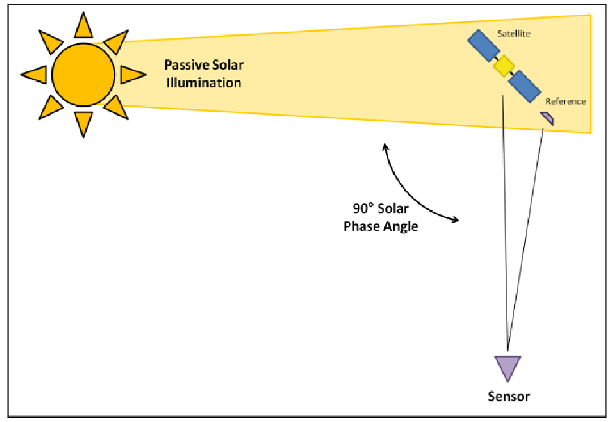

Figure 3: Bistatic scenario showing illumination vector, sensor vector, and solar phase angle

Table 1: Oculus-ASR position descriptions, satellite rotations, and filters used [0=broadband, 4=650nm, 10=I-band, 11V-band, P=polarized]

Position	Description	Rotations	Filters
1	Wings secured down Vertical (90° EL)	5° about nadir Glint map	0, 4, 10, 11 10
2.1	Wings deployed Vertical (90° EL)	5° about nadir	0, 4, 10, 11, 4p, 10p, 11p
2.2	Wings deployed 60° EL	5° about nadir	0, 4, 10, 11, 4p, 10p, 11p
3	Wings deployed Horizontal (0° EL)	Glint map	10
4	Wings deployed Horizontal (0° EL) 13.2° AZ Top SP at glint position	5° about nadir 15° about nadir	4, 10, 11 0, 4
5.1	Wings deployed Horizontal (0° EL) 18° AZ	10° about sensor	0, 4, 10, 11, 4p, 10p, 11p
5.2	Wings deployed Horizontal (0° EL) 13.2° AZ	10° about sensor	0, 4, 10, 11
6	Wings deployed 30° EL 13.2° AZ	5° about nadir	0, 4
7	Wings deployed 45° EL 13.2° AZ	5° about nadir 15° about nadir	10, 11 4p, 10p, 11p
8	Wings deployed 60° EL 13.2° AZ	15° about nadir	0, 4, 10, 11, 4p, 10p, 11p
9	Wings deployed Horizontal (0° EL) 45° AZ	5° about nadir	0, 4, 10, 11
10	Wings deployed 45° EL 45° AZ	90° about nadir	0-11, 0p-11p

Far-field spectral data were collected using an off-axis parabolic mirror. This method was used to collect Oculus-ASR spectra into the ASD sensor. The sensor was placed in the BIS configuration, as was done with the PIXIS imager. Strong glints from satellite surfaces were able to be collected with minimal noise, but off-specular signals were quite noisy.

Measurement Approach and Analysis Methodology

The measurement approach is to have a reference in the scene with every measurement. The object data is then normalized to this reference data under the same lighting conditions. The normalized result is scaled to OCS (m^2) by accounting for object and reference pixel area. The result is directly comparable to simulations performed in TASAT. In the case of the PIXIS images, the object and reference are both in the scene and data are collected simultaneously. Illumination and atmospheric variation in the source such as clouds is divided out. However, in the case of the ASD measurements, the object data and the reference data are acquired sequentially. So any illumination or atmospheric variation between the two measurements results in an error.

A dark current image of the PIXIS noise was taken. Along with the normalization to the reference radiance in the scene, this noise image is subtracted out of the actual satellite imagery in the post-processing to produce normalized and background subtracted images. The normalized (and background subtracted) image is referred to as Unit Irradiance Imagery (UII) which is representative of data obtained under uniform solar illumination. Since measurements made at the optical facility simulate ideal solar illumination conditions, the UII can be used to accurately estimate the OCS of the Oculus-ASR satellite. The OCS measurement is the average unit irradiance image relative to 1 square meter of Spectralon.

ASD measurements are also converted to a comparable OCS measurement in order to directly compare to the PIXIS data. Both the reference and Oculus-ASR spectral data set is normalized to its respective integration time and gain values. Then the theoretical value of the reference relative to Spectralon, if the reference is the glass panel, is calculated based on the geometry of the measurement setup. Finally, the measured Oculus spectral data is normalized by the measured spectral reference data and scaled to the theoretical reference data relative to Spectralon. This final OCS value is now directly comparable to the PIXIS and TASAT imagery.

Using bistatic OCS data of the Oculus-ASR satellite and monostatic OCS data of three colored satellite material coupon samples, a spectral correlation study was performed. The study involved correlating spectral satellite data with spectral coupon data. The spectral angle between the satellite and the coupon data can be determined from the spectral dot product. That is, a data vector with an I-band element, V-band element, and a 650nm element is tied to each coupon sample and to each satellite rotation. The dot product is then calculated between each satellite rotation vector and each coupon sample vector. The nearer the spectral angle was to zero for a given coupon, the larger the contribution of that coupon is to the OCS. This correlation study may help determine Oculus-ASR pose based on correlation between colored panel OCS spectra and coupon data.

RESULTS

Documentation Photos

Several documentation photos of Oculus-ASR were taken over the entire data collection time period which lasted approximately a month. The documentation photos proved valuable during the data analysis as well as during the building of the 3D satellite model. Note that the model will be discussed in a later section in more detail. **Error! Reference source not found.**4 shows two documentation photos of the Oculus-ASR satellite, one with the colored panels secured in the down position and one with the colored panels deployed. Note that only the white panel which is visible in the left side of **Error! Reference source not found.**4 is colored on both sides; the other side panels in the non-deployed configuration are solar panels while the underside is colored anodized aluminum.

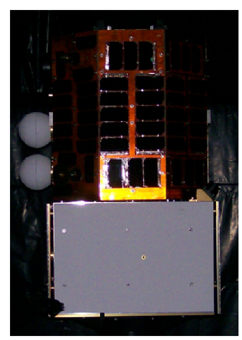

(a)

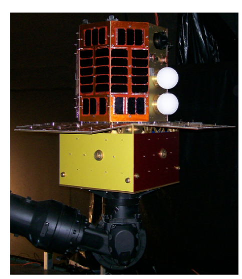

(b)

Figure 4: Documentation photos of Oculus-ASR where the side panels are (a) secured down and (b) deployed

PIXIS Imagery

Error! Reference source not found.5 shows PIXIS imagery for satellite rotations of 20° (off-glint), 90° (octagon glint), and 135° (octagon and base glint) in the I-band for two positions, position 1 with the panels secured down and position 2 with the panels deployed. Note that because of the choice of reference material (based on the satellite radiance), the image scaling is different between the first image and the next two images. Because of the large dynamic range between the glint and off-glint rotations, both glass and Spectralon were used as references. These PIXIS images are used to calculate the OCS data that follows.

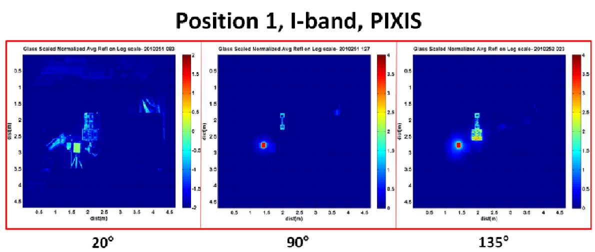

(a) Position 1

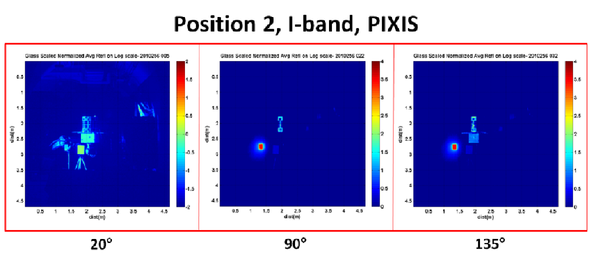

(b) Position 2

Figure 5: PIXIS I-band images at three rotation angles for two positions

OCS results for the satellite while in position 2 (see **Error! Reference source not found.** for position description) are shown in **Error! Reference source not found.**6 for all wavebands. Note that in position 2, the colored panels on the base of Oculus-ASR are deployed. For rotation angles of 45°, 135°, and 315°, both the colored panel and the top solar panel glint; for rotation angle 225°, only the red colored panel glints. The solar panel peak glints (0°, 90°, 180°, and 270°) are not resolved and the solar panel glint width is smaller than that for the colored panels. This is evident in this plot.

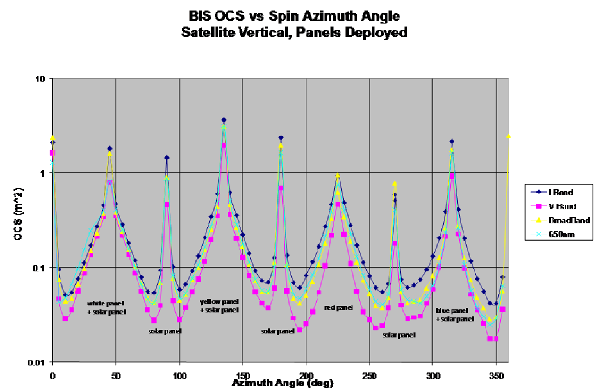

Figure 6: PIXIS OCS data for position 2 in all 4 wavebands

It is not likely for ground-based telescopes to observe sharp solar panel glints unless special efforts are made to align the satellite appropriately. More likely geometries are off-glint positions where the satellite is not completely nadir-pointing, as in position 2.2. Please note the glyph in the top right corner of **Error! Reference source not found.**7. In some figures, the glyph has been transposed so the illumination angle is different. This does not affect the analysis. OCS results for the Oculus-ASR satellite while in position 2.2 are shown in **Error! Reference source not found.**7. Because the geometry is off-specular, the OCS values are less than 0.1m^2. The visible colored panel is labeled in the figure. Sharp solar panel glint contributions are not apparent in this position; the four peaks in the plot are associated with the colored panels.

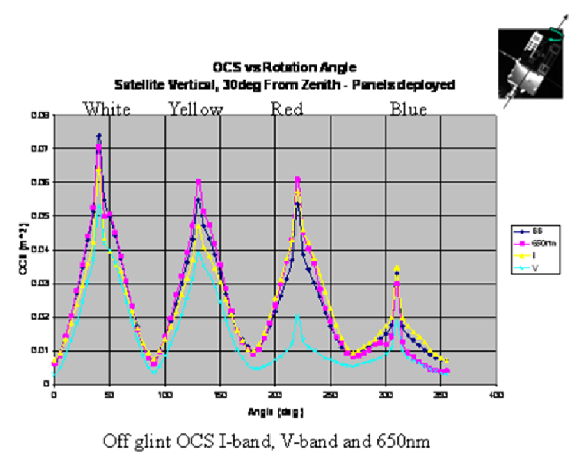

Figure 7: OCS values as a function of spin azimuth and waveband for position 2.2

Error! Reference source not found.8 shows OCS values for the Oculus-ASR satellite in position 10. Note the double reflection shown in the glyph between the colored side panel and the base. The OCS values in the figure are for 11 wavebands and for 4 satellite rotations. The top and left colored panels are indicated (R=red, W=white, Y=yellow, B=blue) as these panels contribute prominently to the OCS. For this geometry, the spin azimuth could be determined if observations were made in wavebands that may distinguish the colors better such as 488nm, 532nm, 650nm or a red-green-blue (RGB) color scheme. Please note that this data is similar to the coupon data obtained, which will be discussed in a later section of the Results chapter.

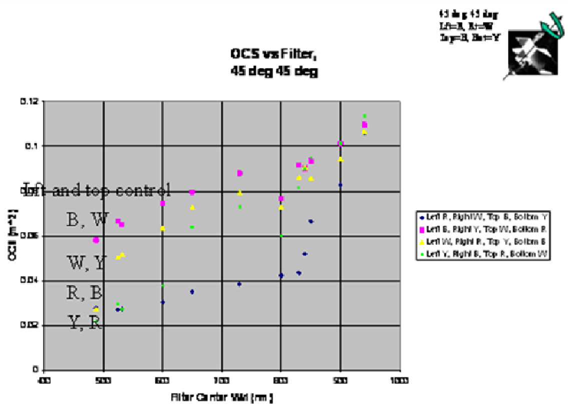

Figure 8: OCS values as a function of waveband for 4 satellite rotations which are indicated

Two deployable calibration spheres are attached to the Oculus-ASR satellite. A short experiment was performed to investigate the contribution to the OCS of the deployable spheres. **Error! Reference source not found.**9 shows I-band and V-band results comparing the satellite OCS (top row images) with the sphere OCS (bottom row images). The OCS value of the satellite is an order of magnitude larger than that of the sphere indicating that the contribution made to the satellite OCS by the sphere is minute.

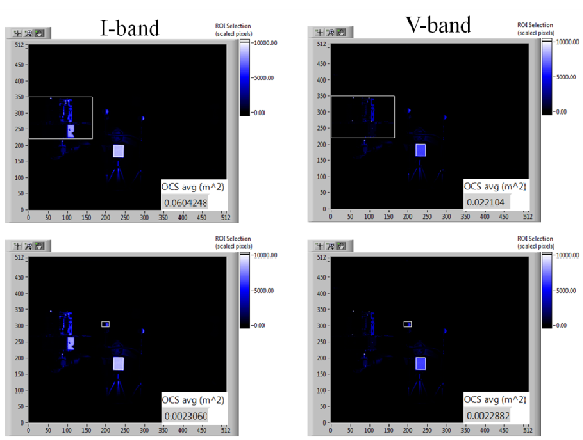

Figure 9: OCS contribution comparison for the sphere deployment experiment. I-band and V-band data are shown.

ASD Spectral Data

Far-field spectral OCS data of Oculus-ASR was attempted using an off-axis parabolic mirror. Solar panel spectra were acquired; colored panel spectra were observed but extremely noisy. While the satellite was in position 3 (see **Error! Reference source not found.**), the top solar panel spectrum was acquired and is shown in **Error! Reference source not found.**10. Characteristic spectral variation of a solar panel absorption spectrum is evident in the visible bands as well as a characteristic flat spectrum in the short-wave infrared bands.

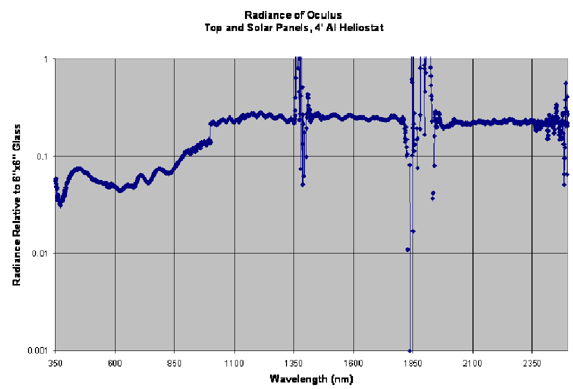

Figure 10: Oculus-ASR top solar panel spectrum relative to the glass reference

Pose Determination from Spectral Dot Product

Monostatic OCS data of the red, blue, and yellow coupon samples was acquired in the I-band, V-band, and at 650nm. A documentation photo of the three colored anodized aluminum samples is shown in **Error! Reference source not found.**11. Using this coupon data and the full rotation Oculus-ASR OCS data acquired while the satellite is in position 2.2 (**Error! Reference source not found.**7) for the same wavebands, the spectral dot product is calculated in order to determine satellite pose.

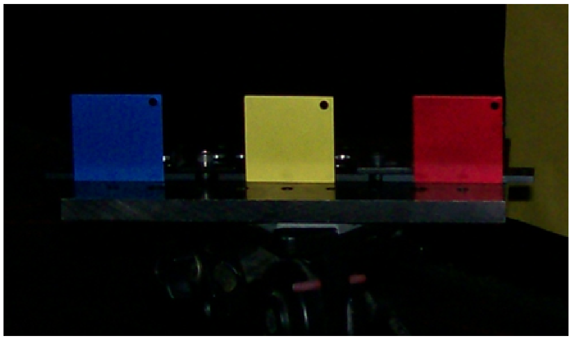

Figure 11: Documentation photo of the R, B, and Y coupon samples

The spectral angles or correlations are shown in **Error! Reference source not found.**2. As seen in the figure, when the red coupon serves as the reference (the red line), the spectral angle is minimum when the red panel is prominent on the satellite. Similarly, the spectral angle when the blue coupon is used is minimum when the blue panel is prominent. In further examination of the plot, when the yellow coupon is used as a reference, there are a few minimums suggesting that the yellow-gold reflection of the satellite bus rather than just the yellow colored panel is influencing the results. Also as seen in the figure, the yellow coupon reference correlates strongly with the white panel. Because of the choice of filter bands, the discrimination between the yellow, red, and blue panels is not good.

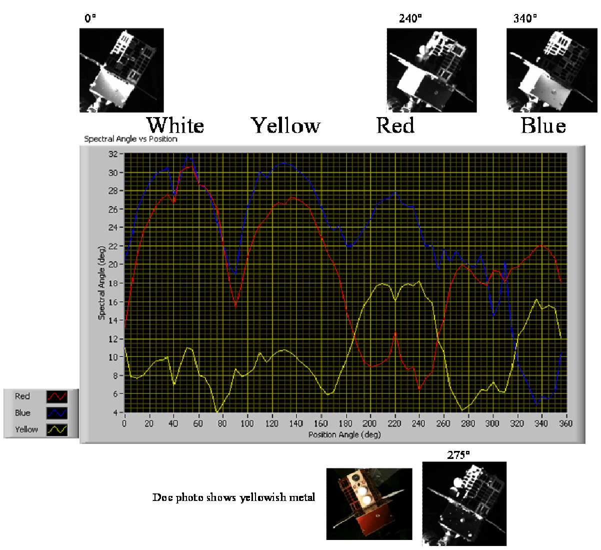

Figure 12: Spectral angle dot product results (red, blue, and yellow BRDF vectors dotted with OCS V, I, and 650nm filter vector) as a function of spin azimuth for position 2.2

TASAT MODELING AND SIMULATION

Several different predictive models of the Oculus-ASR satellite were built for use in TASAT. The models were built using engineering diagrams, documentation photos, and visual inspection of the satellite. A total of four models were built, with different features on each. The first and second models have the wing panels secured down, both with and without the deployable spheres attached. The second and third models have the wing panels deployed, both with and without the spheres attached. The left side of **Error! Reference source not found.**3 shows a rendered image of the satellite model with the colored wing panels secured down and the sphere deployed; the right side of the figure shows a rendered image of the satellite model with the wings deployed but the spheres attached. These renderings were generated directly from the 3D satellite model.

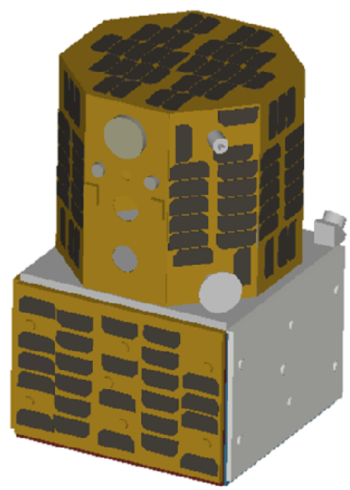

(a)

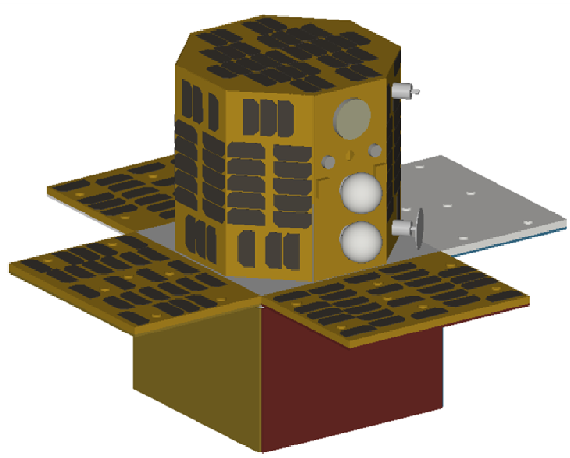

(b)

Figure 13: Rendered Oculus-ASR satellite 3D models with (a) wings secured down, no spheres and (b) wings deployed, with spheres

Error! Reference source not found.4 shows the material breakdown on two of the models. The materials used on the model are shown in decreasing order of percent contribution to the surface area given the orientation. The materials were selected based on a description of the materials visible on the satellite. Note that two additional models were built similar to this, the only difference being that the spheres were removed. The same materials were used for those models as well.

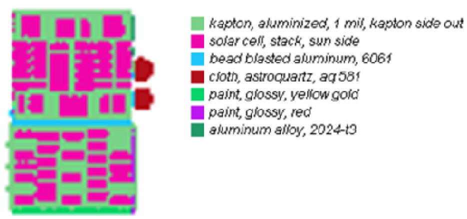

(a) Wings secured down

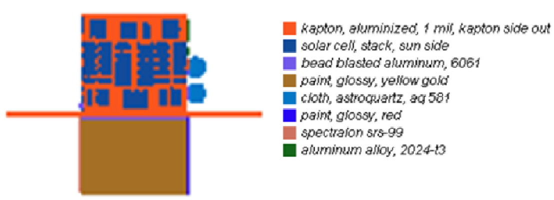

(b) Wings deployed

Figure 14: Oculus-ASR model showing two different wing configurations, but both with the spheres attached

TASAT simulations were conducted in order to compare predicted imagery with the ground truth imagery. The satellite was "posed" in TASAT to simulate facility measurement geometries. The same wavebands were also used in the simulations. The simulated OCS data for all wavebands is shown in **Error! Reference source not found.**5. Eight strong glints are prominent in the plot corresponding to the solar panel glints. The strongest glints represent the reflection from the solar panels on the octagonal structure and the solar panels on the base. The weaker glints correspond to only glints from the octagon, as the base was at a corner at these rotation angles.

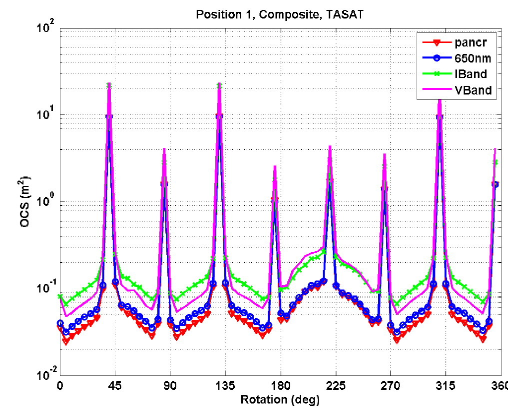

Figure 15: TASAT simulated imagery of Oculus-ASR in position 1

CONCLUSIONS

A successful ground-truth characterization experiment was performed on the Oculus-ASR satellite. Optical signatures of the satellite were acquired which were then used to build the 3D predictive satellite models. Based on the accurate imagery and glint and off-glint ground truth datacollected, the predictive models were validated and improvements were made to the simulation and materials database in order to improve simulated and ground truth optical satellite signature agreement.

It is concluded that determination of which colored panel of the Oculus-ASR is most visible from on-orbit spectral data is plausible upon analysis of ground truth data. Pose determination can then be estimated based on the most prominent colored panel visible. However, the current satellite material choices and the chosen wavebands that data was acquired in were not optimum. One change that may improve spectral signature collection and pose determination would be to change the panel colors from red, yellow, and blue, to red, green, and blue. The spectral difference between these colors is greater than the first set of colors. Also, using more diffuse materials such as a diffuse colored paint may provide larger signals at non-specular geometries. The choice of wavebands to acquire data in was not optimum. RGB 50nm FWHM filters would work best with the recommended panel color change. Additionally, a polarizer may remove much of the first surface reflection which will increase the difference in spectral signal among wavebands.

The objectives of the Oculus-ASR mission stated in the introduction were successfully completed. A ground-truth characterization of the spacecraft was performed to aid in the understanding of space object signatures for SSA. Based on the ground-truth characterization data, successful construction and validation of predictive computer models was accomplished. And an investigation in pose determination from on-orbit spectral returns was performed.

ACRONYMS

AFRL	Air Force Research Laboratory
ASR	Attitude & Shape Recognition
AZ	Azimuth
BIS	Bistatic
BCS	Body Coordinate System
BRDF	Bidirectional Reflectivity Distribution Function
EL	Elevation
MTU	Michigan Technological University
OCS	Optical Cross Section
SSA	Space Situational Awareness
TASAT	Time-domain Analysis Simulation for Advanced Tracking
UNP	University Nanosatellite Program

ACKNOWLEDGEMENTS

The Oculus-ASR team would like to extend their thanks to AFRL who provided facilities to make the necessary optical measurements and to perform the predictive modeling. The team would also like to acknowledge the generous sponsors that have supported the project, including:

ABSL Power Solutions
Air Force Research Laboratory
Air Force Office of Scientific Research
Altia
Analog Devices
AMP Netconnect
AGI
Bartington Instruments
C&R Technologies
Connect Tech Incorporated
Dunmore Corporation
Integrity Applications Incorporated
Mathworks
Michigan Space Grant Consortium
PCB Piezotronics
Raytheon Missile Systems
SAIC
Systems Integration Plus Incorporated
TiNi Aerospace
Tyco Electronics
Wind River